Invited Paper

Techniques for sensitive measurements of gravitational acceleration using single state echo atom interferometers

G. Carlse, J. Randhawa, A. Pouliot, T. Vacheresse, E. Ramos, and A. Kumarakrishnan
Department of Physics and Astronomy, York University, Toronto, Ontario, Canada M3J 1P3

ABSTRACT

Given the prominent role which atom interferometers play in the emerging fields of quantum-based navigation and remote sensing, we discuss schemes for velocimetry and accelerometry using a single-state atom interferometer. These techniques rely on momentum state interference arising from the application of a standing-wave optical excitation pulse on a laser-cooled atomic sample falling in a gravitational field. Kapitza-Dirac diffraction of momentum-states leads to the formation of a density modulation (or grating) in the atomic ground state. Motional properties of the sample, including the local value of gravitational acceleration (g), are encoded in the grating as it falls and can be imprinted on a backscattered travelling wave read-out field. Since these gratings dephase according to their velocity distribution, the grating free-induction decay (FID) may be probed immediately after the excitation. Alternatively, a grating-echo, which is read-out in the vicinity of $t = 2T_{21,}$ can be realized by applying a second sw pulse at a time $t = T_{21}$. We review grating-echo techniques for velocimetry and accelerometry that have achieved precision in g determinations at the level of 50 parts per billion and efforts to improve the signal size by increasing the grating contrast. We also describe a single-state velocimeter based on measurement of the FID that has achieved velocity sensitivity at the level of 600 μm/s and determinations of g with a precision of 2 mm/s^2. These simple techniques have the potential to realize the most precise velocimeter due to their limited susceptibility to phase interruptions, despite use over long timescales.

Keywords: Atom Interferometry, Precision Metrology, Laser Cooling and Trapping of Neutral Atoms, Atom Optics, Inertial Effects, Gravimeters, Coherent Transient Effects, Velocimetry

1. INTRODUCTION

The development of inertial sensing techniques using ultracold atoms is of great importance for precise tests of fundamental physical laws [1-3], as well as for the development of robust platforms for navigation and remote sensing [4-7]. In this field, quantum metrology has been gaining, and in many cases, exhibiting the potential for surpassing analogous classical techniques. This trend is particularly apparent in measurements of velocity and acceleration, for which atom based quantum sensors have become the basis for state of the art measurement [8,9]. The workhorse among these devices are Raman atom interferometers [10] (AIs) which have been employed to measure several classes of inertial effects with great success [11-17]. These AIs rely on the wave nature of matter which emerges at extremely low temperatures characteristic of laser-cooled atoms and precisely timed laser pulses to manipulate atoms between hyperfine levels. The experiments require exquisite control of the frequencies of excitation lasers to ensure two photon optical excitation of atoms.

The focus on developing Raman AIs has overshadowed the potential of a separate class of single state AIs that can measure many of the same phenomena with much simpler technical requirements [18-20]. Rather than manipulating atoms between hyperfine levels, these AIs rely on the interference of atoms with different momentum states associated with the same atomic ground state. As a result, the AI requires only one laser system, and through the use of echo techniques, it can avoid the need for velocity selection. By virtue of their simplicity, single-state AIs also exhibit the potential to limit systematic effects due to level shifts arising from electric and magnetic fields. Accordingly, they offer promising and robust alternatives for inertial measurements.

2. SINGLE-STATE ECHO ATOM INTERFEROMETERS

The principle behind a single-state AI relies on recording the contrast of an atomic grating formed in the ground state of a laser cooled atomic sample. The atomic grating is formed due to the Kapitza-Dirac diffraction due to excitation by counter-propagating laser fields that constitute a standing-wave (sw). In this manner, atoms undergo a two-photon

Quantum Sensing, Imaging, and Precision Metrology III, edited by
Selim M. Shahriar, Proc. of SPIE Vol. 13392, 1339204 · © 2025
SPIE · 0277-786X · doi: 10.1117/12.3053203

transition which creates a sample in a superposition of momentum states separated by $2\hbar k$, where $k = 2\pi/\lambda$ is the wavevector of the excitation field. In a classical description, this is akin to the atoms being pushed towards the nodes of the sw potential which has a periodicity of $\lambda/2$, where λ is the wavelength of the excitation. In a quantum picture, the resulting matter-wave interference results in a periodic density modulation of the atomic ground state.

Since the source of the grating is the interference of momentum states, its contrast dissipates due Doppler dephasing, known as a free-induction decay (FID). The thermal speed of the sample limits the timescale of these measurements to a few microseconds for cold atomic samples with temperatures of a few microKelvin. This timescale can be extended through the use of echo techniques, where the application of second sw pulse at a time T_{21} after the first excitation, results in the reformation of the grating contrast at the echo time $t = 2T_{21}$, as shown in Figure 1a.

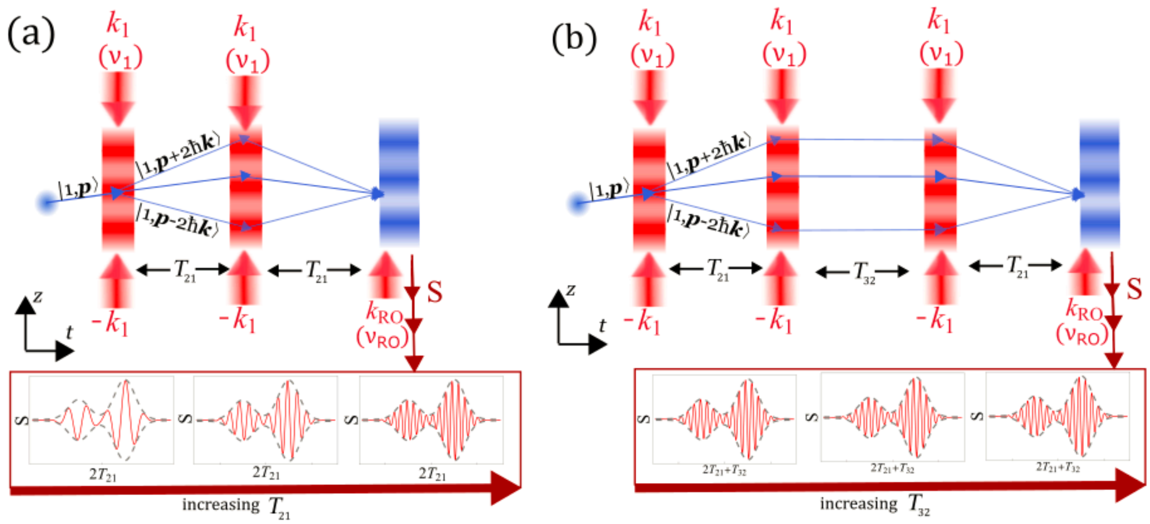

Figure 1. (a) Pulse sequence for the single-state echo interferometer with resulting momentum state interference of a generic state $|1,\mathbf{p}\rangle$ and grating formation shown in purple. The sw excitation is indicated by wavevectors $\pm k_1$, while the read-out field is shown by k_{RO}, and the scattered field is shown by S. The lower panel shows the scattered field signal envelope (dashed lines) and signal phase (solid lines) near the echo time $2T_{21}$. From left to right are shown examples for increasing pulse separations (T_{21}). (b) Shows the same information for a three pulse single-state echo interferometer velocimeter, where the lower panel shows the scattered field signal envelope (dashed lines) and signal phase (solid lines) near the echo time $2T_{21}+T_{32}$. From left to right are shown examples for increasing pulse separations (T_{32}).

This density modulation can be conveniently read-out by back scattering a traveling wave readout field that is nearly resonant with the excited state and turned on in the vicinity of the echo time. The amplitude and phase of the grating at the time of this read-out pulse is imprinted onto the backscattered signal envelope (see Figure 1). Despite the FID, as the atoms in the grating evolve, they will accumulate a quantum mechanical phase associated with the atomic recoil resulting from the two-photon interaction with the sw. This property of the AI has been used to demonstrate a measurement of the recoil frequency [18,21,22]. In addition to the recoil phase, the grating will also accumulate a phase resulting from a local gravitational field. By varying the time separation between excitation pulses and measuring the average phase across the echo envelope, it is possible to measure the chirped accumulation of gravitational phase, which will vary as gT_{21}^2, where g is gravitational acceleration.

In this manner, g can be measured using suitably long observation times [18,20,23,24]. The essential characteristic of the two-pulse AI is that the different momentum states comprising the arms of the interferometer experience a continuously changing relative displacement during the entire experiment. The signal from the AI is analogous to the interference fringes recorded by the falling corner-cube optical interferometer in Ref. [25].

The best demonstration of the two-pulse technique to measure g utilized a sample with a temperature of ~20 uK, that was dropped over a distance of ~1 cm and achieved a precision of ~7 ppm [20,23]. Here the signal size of the single-state echo-type AI, which is ~1 photon per atom, was further restricted by magnetic gradients, and the transverse expansion of the atomic sample beyond the radius of the excitation beams. Additionally, since the apparatus was only passively isolated from mechanical vibrations, phase measurements were compromised on timescales greater than 10 ms.

Recently, there have been efforts to improve the contrast of these echo gratings using optical channeling pulses [26] and optimized readout pulses [27], which appear promising for increasing the signal size and extending the experimental timescale. Similarly, other AIs have employed a combination of active vibration isolation and signal correction showing results [28]. There has also been a growing interest in atomic velocimetry which has exhibited a greater resilience to mechanical vibrations [29]. This advantage has to be weighed against their inherent limitation that the phase accumulation in a gravitational field scales as T_{21} as opposed to the T_{21}^2 scaling of accelerometers. This limitation applies to echo AIs as well.

A simple way to realize a velocimeter with the single-state echo-type AI is by altering the optical pulse sequence. As shown in Figure 1b, the addition of a third sw pulse will enable a "stimulated-echo" configuration [30]. Here, the first sw pulse creates a superposition of momentum states separated by $2\hbar k$. A second SW pulse applied at $t = T_{21}$ results in momentum states that are copropagating at fixed separation with the same momentum. A third pulse applied at $t = T_{21} + T_{32}$ causes the copropagating states to interfere at the echo time $t_{\text{echo}} = 2T_{21} + T_{32}$, forming a density grating. As in the two-pulse AI, the grating formation is associated with interference of momentum states separated by $2\hbar k$. The theory of this interferometer was described in detail in Ref. [31] and predictions were verified using measurements of magnetic field gradients that did not require vibration stabilization.

During the central pulse separation (T_{32}), the arms of the three-pulse AI consist of copropagating wave packets with no momentum difference, accordingly, the amplitude of the echo envelope shows no recoil modulation as a function of T_{32}. However, the phase of the echo is modulated at a fixed frequency which can be shown to be $2kgT_{21}$. Naturally, this configuration represents a velocimeter since the frequency is determined by the velocity gT_{21} which the atoms acquire during the time interval T_{21} due to gravity. The sinusoidal period of the echo phase as a function of T_{32} is given by $\tau_v = gT_{21}\lambda/2$. Thus, by varying this separation T_{32}, a measurement of the center-of-mass velocity of the sample is equally possible, and repeated measurements of this with different initial pulse separations (T_{21}) can be used to measure g. Indeed, the most sensitive echo-type AI measurement of g has been performed using this scheme with a precision of 75 ppb and a drop height of 1 cm [23].

An even simpler scheme to extract the instantaneous center-of-mass velocity involves measuring the Doppler phase across the echo envelope (dashed lines in Figure 1) in either two-pulse or three-pulse AIs, as in Ref [23]. Here, a phase change of 2π indicates that the grating has fallen through a single period of the optical potential ($\lambda/2$), an effect that has been used to determine g at the level of 1% by repeating measurements by incrementing the values of T_{21} or T_{32}.

3. SINGLE-STATE GRATING VELOCIMETRY

The simplest form of single-state velocimeter does not employ the echo technique at all. Rather it leverages the initial matter-wave interference which follows the application of a single excitation pulse. The contrast of the atomic grating can be made velocity dependent by detuning the two travelling wave components of the sw excitation [32]. The ensuing grating contrast will have a maximum when the two components have the same frequency in the frame of reference of the moving atomic sample, falling off as: $C \propto \sin^2(\tau\ (\nu_2 - \nu_1))/(\tau\ (\nu_2 - \nu_1))$, where ν_1 and ν_2 are the two excitation components in the laboratory frame and τ is the pulse duration.

First order Doppler shifts are easily discernible as frequency shifts of the central maximum if the contrast spectrum is recorded at different drop times. Thus, center of mass velocimetry and accelerometry can be performed by tracking this line center. While it is possible to narrow this line by elongating the excitation pulse duration, as is Raman velocimetry [33], it is more advantageous to narrow this spectrum using a time-separated oscillatory fields (TSOF) or Ramsey method [34], where complications arising from optical channeling can be avoided. In this configuration, two sw pulses with durations τ are applied at a time separation T, resulting in a contrast spectrum which has the form: $C \propto (A+2D\cos^2(T_{\text{eff}}(\nu_2 - \nu_1)/2+\phi_l)^2-1)\ \sin^2(\tau\ (\nu_2 - \nu_1))/(\tau\ (\nu_2 - \nu_1))$, where $T_{\text{eff}} = T + \tau$ is the time between the center of the two sw pulses. Here, A is a proportionality constant and D is a unitless parameter which describes the FID of the atomic grating. There is also a phase shift ϕ_l, accounting for differences in the phase of the two excitation pulses. The resulting narrowed fringe allows for measurements of velocity at the coherence limit of the cold samples in question. Tracking the Doppler shift of the Ramsey fringe as a function of the drop time, results measurements of velocity with a sensitivity of 600 μm/s and determinations of g with a precision of 2 mm/s^2 [32].

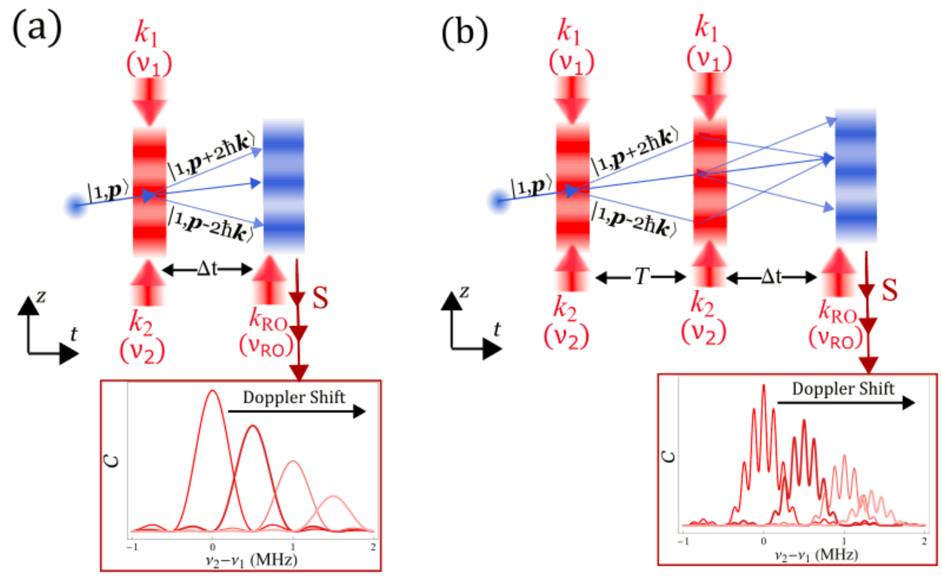

Figure 2 (a) Pulse sequence for the single-state grating velocimeter with the resulting momentum state interference of a generic state $|1,\mathbf{p}\rangle$ and the formation of the atomic grating shown in purple. The sw excitation is indicated by wavevectors k_1 and k_2, while the read-out field is shown by k_{RO}, and the scattered field is shown by S. The lower panel shows the signal contrast as a function of the relative detuning between the two excitation beam components (k_1 and k_2) with frequencies ν_1 and ν_2. Center-of-mass velocity of the sample is manifested as a horizontal Doppler shift of the spectrum. Such a Doppler shift can be observed by increasing the drop time (b) Shows the same as (a) but for the TSOF velocimeter where a Ramsey fringe is imprinted on the contrast spectrum by applying two sw pulses separated by a time interval T. In both figures, the readout pulse is applied immediately after the final sw excitation. However, in Figure 2a, the onset of the readout pulse is indicated by the time delay Δt $<< T$, which is exaggerated to show the momentum state interference.

These techniques which rely only on measuring the magnitude of the grating contrast avoid the problem of monitoring the phase of the backscattered field and the phases of the excitation beams. The reduced complexity latter is enabled since the FID signal, unlike the echo counterpart, is only observable over the coherence time of the cold sample which is an order of magnitude smaller than the timescale for the onset of mechanical vibrations.

4. FUTURE DIRECTIONS

Since this technique is ultimately limited by the coherence of the sample it is reasonable to consider how well the TSOF velocimeter will perform in alternative samples with longer coherence times. As they are now fairly widely used, we consider here the case of a typical Bose gas [35,36]. In such a sample, where the coherence time is on the order of hundreds of microseconds, much larger pulse separations will be possible. In these proposed experiments one could conceivably measure frequency shifts on the order of several kiloHertz representing a velocity sensitivity of less than 10 μm/s, which greatly surpasses all other cold atom velocimeters and challenges the precision obtained by the most precise atomic velocimeter [33]. Similarly, velocimetric measurements of g would also be enhanced by use of these long timescales. When combined with long observation times achievable in drop towers [37,38], measurements of g at the level of 10 parts per billion (ppb) may also be possible. These are particularly appealing measurements, since despite the use of extraordinarily long drop times of order 1 s [39], possible in such towers, the phase stability of the AI will only need to be maintained over the coherence time of the cold sample (~ a few milliseconds).

In tabletop experiments however, the echo-type AI is capable of significantly improved performance. As previously noted, efforts to improve the reflectivity of the gratings [26,27] show promise for extending the measurement timescale so that the drop heights can exceed ~ 30 cm (250 ms). In combination with efforts to both passively and actively stabilize the apparatus, the precision of echo techniques can be expected to scale up to the ppb level. However, like conventional

Raman AIs, it will be necessary to monitor the phase of the AI pulses, since phase stability will be required over the entire drop interval.

ACKNOWLEDGEMENTS

This work was supported by the Canada Foundation for Innovation, the Ontario Innovation Trust, the Ontario Centers of Excellence, the Natural Sciences and Engineering Research Council of Canada (NSERC), York University, and the Helen Freedhoff Memorial Fund. We also acknowledge helpful discussions with Louis Marmet of York University.

REFERENCES

[1] Tarallo, M. G., Mazzoni, T., Poli, N., Sutyrin, D. V., Zhang, X., and Tino, G. M., "Test of Einstein equivalence principle for 0-spin and half-integer-spin atoms: Search for spin-gravity coupling effects," Phys. Rev. Lett. 113, 023005 (2014).

[2] Overstreet, C., Asenbaum, P., Kovachy, T., Notermans, R., Hogan, J. M., and Kasevich, M. A., "Effective inertial frame in an atom interferometric test of the equivalence principle," Phys. Rev. Lett. 120, 183604 (2018).

[3] Asenbaum, P., Overstreet, C., Kim, M., Curti, J., and Kasevich, M. A., "Atom-interferometric test of the equivalence principle at the 10^{-12} level," Phys. Rev. Lett. 125, 191101 (2020).

[4] Barrett, B., Antoni-Micollier, L., Chichet, L., Battelier, B., L´eveque, T., Landragin, A., and Bouyer, P., "Dual matter-wave inertial sensors in weightlessness," Nature Communications 7(1), 13786 (2016).

[5] Battelier, B., Barrett, B., Fouché, L., Chichet, L., Antoni-Micollier, L., Porte, H., Napolitano, F., Lautier, J., Landragin, A., and Bouyer, P., "Development of compact cold-atom sensors for inertial navigation," in [Quantum Optics], Stuhler, J. and Shields, A. J., eds., 9900, 990004, International Society for Optics and Photonics, SPIE (2016).

[6] Bidel, Y., Zahzam, N., Blanchard, C., Bonnin, A., Cadoret, M., Bresson, A., Rouxel, D., and Lequentrec-Lalancette, M., "Absolute marine gravimetry with matter-wave interferometry," Nature Communications 9(1), 627 (2018).

[7] Bidel, Y., Zahzam, N., Bresson, A., Blanchard, C., Cadoret, M., Olesen, A. V., and Forsberg, R., "Absolute airborne gravimetry with a cold atom sensor," Journal of Geodesy 94, 1–9 (2020).

[8] Peters, A., Chung, K. Y., and Chu, S., "Measurement of gravitational acceleration by dropping atoms," Nature 400(6747), 849–852 (1999).

[9] Chen, Z., Lim, H. M., Huang, C., Dumke, R., and Lan, S.-Y., "Quantum-enhanced velocimetry with Doppler-broadened atomic vapor," Phys. Rev. Lett. 124, 093202 (Mar 2020).

[10] Kasevich, M. and Chu, S., "Atomic interferometry using stimulated Raman transitions," Phys. Rev. Lett. 67, 181–184 (1991).

[11] Hu, Z.-K., Sun, B.-L., Duan, X.-C., Zhou, M.-K., Chen, L.-L., Zhan, S., Zhang, Q.-Z., and Luo, J., "Demonstration of an ultrahigh-sensitivity atom-interferometry absolute gravimeter," Phys. Rev. A 88, 043610 (2013).

[12] McGuirk, J. M., Foster, G. T., Fixler, J. B., Snadden, M. J., and Kasevich, M. A., "Sensitive absolute- gravity gradiometry using atom interferometry," Phys. Rev. A 65, 033608 (2002).

[13] Snadden, M. J., McGuirk, J. M., Bouyer, P., Haritos, K. G., and Kasevich, M. A., "Measurement of the earth's gravity gradient with an atom interferometer-based gravity gradiometer," Phys. Rev. Lett. 81, 971–974 (1998).

[14] Rakholia, A. V., McGuinness, H. J., and Biedermann, G. W., "Dual-axis high-data-rate atom interferometer via cold ensemble exchange," Phys. Rev. Appl. 2, 054012 (2014).

[15] Gustavson, T., Landragin, A., and Kasevich, M., "Rotation sensing with a dual atom-interferometer sagnac gyroscope," Classical and Quantum Gravity 17(12), 2385 (2000).

[16] Canuel, B., Leduc, F., Holleville, D., Gauguet, A., Fils, J., Virdis, A., Clairon, A., Dimarcq, N., Bordé, C. J., Landragin, A., and Bouyer, P., "Six-axis inertial sensor using cold-atom interferometry," Phys. Rev. Lett. 97, 010402 (2006).

[17] Wu, X., Pagel, Z., Malek, B. S., Nguyen, T. H., Zi, F., Scheirer, D. S., and Müller, H., "Gravity surveys using a mobile atom interferometer," Science Advances 5(9), eaax0800 (2019).

[18] Cahn, S. B., Kumarakrishnan, A., Shim, U., Sleator, T., Berman, P. R., and Dubetsky, B., "Time-domain de Broglie wave interferometry," Phys. Rev. Lett. 79, 784–787 (1997).

[19] Barrett, B., Chan, I., Mok, C., Carew, A., Yavin, I., Kumarakrishnan, A., Cahn, S. B., and Sleator, T., "Time-domain interferometry with laser-cooled atoms," in [Advances in Atomic, Molecular, and Optical Physics], 60, 119–199, Elsevier (2011).

[20] Barrett, B., Carew, A., Beica, H. C., Vorozcovs, A., Pouliot, A., and Kumarakrishnan, A., "Prospects for precise

measurements with echo atom interferometry," Atoms 4(3), 19 (2016).
[21] Barrett, B., Carew, A., Beattie, S., and Kumarakrishnan, A., "Measuring the atomic recoil frequency using a modified grating-echo atom interferometer," Phys. Rev. A 87, 033626 (2013).
[22] Beattie, S., Barrett, B., Weel, M., Chan, I., Mok, C., Cahn, S. B., and Kumarakrishnan, A., "Influence of spontaneous emission on a single-state atom interferometer," Phys. Rev. A 77, 013610 (2008).
[23] Mok, C., Barrett, B., Carew, A., Berthiaume, R., Beattie, S., and Kumarakrishnan, A., "Demonstration of improved sensitivity of echo interferometers to gravitational acceleration," Phys. Rev. A 88, 023614 (2013).
[24] Weel, M., Chan, I., Beattie, S., Kumarakrishnan, A., Gosset, D., and Yavin, I., "Effect of a magnetic field gradient and gravitational acceleration on a time-domain grating-echo interferometer," Phys. Rev. A 73, 063624 (2006).
[25] Niebauer, T. M., Sasagawa, G. S., Faller, J. E., Hilt, R., and Klopping, F., "A new generation of absolute gravimeters," Metrologia 32, 159 (1995).
[26] Carlse, G., Randhawa, J., Ramos, E., Vacheresse, T., Pouliot, A., Carew, A. C., and Kumarakrishnan, A., "Role of optical channeling in contrast enhancement of echo interferometers," Phys. Rev. A 109, 043307 (2024).
[27] Carlse, G., Randhawa, J., Ramos, E., Vacheresse, T., Pouliot, A., Carew, A. C., Kumarakrishnan, A., and Barrett, B., "Optimization of Bragg scattering from atomic gratings for echo interferometry," Phys. Rev. A 110, 043306 (2024).
[28] Gong, W., Li, A., Huang, C., Che, H., Feng, C., and Qin, F., "Effects and prospects of the vibration isolation methods for an atomic interference gravimeter," Sensors 22(2), 583 (2022).
[29] Su, E. J., Wu, S., and Prentiss, M. G., "Atom interferometry using wave packets with constant spatial displacements," Phys. Rev. A 81, 043631 (2010).
[30] Mossberg, T. W., Kachru, R., Hartmann, S. R., and Flusberg, A. M., "Echoes in gaseous media: A generalized theory of rephasing phenomena," Phys. Rev. A 20, 1976–1996 (1979).
[31] Barrett, B., Chan, I., and Kumarakrishnan, A., "Atom-interferometric techniques for measuring uniform magnetic field gradients and gravitational acceleration," Phys. Rev. A 84, 063623 (2011).
[32] G. Carlse, J. Randhawa, E. Ramos, T. Vacheresse, A. Pouliot, and A. Kumarakrishnan, Velocimetry with matter-wave lattices, Submitted, Physical Review. (2024).
[33] Chabé, J., Lignier, H., Szriftgiser, P., and Garreau, J. C., "Improving raman velocimetry of laser-cooled cesium atoms by spin-polarization," Optics Communications 274(1), 254–259 (2007).
[34] Ramsey, N. F., "A molecular beam resonance method with separated oscillating fields," Phys. Rev. 78, 695–699 (1950).
[35] Gupta, S., Dieckmann, K., Hadzibabic, Z., and Pritchard, D. E., "Contrast interferometry using Bose-Einstein condensates to measure h/m and α," Phys. Rev. Lett. 89, 140401 (Sep 2002).
[36] Jamison, A. O., Plotkin-Swing, B., and Gupta, S., "Advances in precision contrast interferometry with Yb Bose-Einstein condensates," Phys. Rev. A 90, 063606 (2014).
[37] Könemann, T., Brinkmann, W., Göklü, E., Lämmerzahl, C., Dittus, H., Van Zoest, T., Rasel, E., Ertmer, W., Lewoczko-Adamczyk, W., Schiemangk, M., et al., "A freely falling magneto-optical trap drop tower experiment," Applied Physics B 89, 431–438 (2007).
[38] Müntinga, H., Ahlers, H., Krutzik, M., Wenzlawski, A., Arnold, S., Becker, D., Bongs, K., Dittus, H., Duncker, H., Gaaloul, N., Gherasim, C., Giese, E., Grzeschik, C., Hänsch, T. W., Hellmig, O., Herr, W., Herrmann, S., Kajari, E., Kleinert, S., L¨ammerzahl, C., Lewoczko-Adamczyk, W., Malcolm, J., Meyer, N., Nolte, R., Peters, A., Popp, M., Reichel, J., Roura, A., Rudolph, J., Schiemangk, M., Schneider, M., Seidel, S. T., Sengstock, K., Tamma, V., Valenzuela, T., Vogel, A., Walser, R., Wendrich, T., Windpassinger, P., Zeller, W., van Zoest, T., Ertmer, W., Schleich, W. P., and Rasel, E. M., "Interferometry with Bose-Einstein condensates in microgravity," Phys. Rev. Lett. 110, 093602 (2013).
[39] Deppner, C., Herr, W., Cornelius, M., Stromberger, P., Sternke, T., Grzeschik, C., Grote, A., Rudolph, J., Herrmann, S., Krutzik, M., Wenzlawski, A., Corgier, R., Charron, E., Guéry-Odelin, D., Gaaloul, N., Lämmerzahl, C., Peters, A., Windpassinger, P., and Rasel, E. M., "Collective-mode enhanced matter-wave optics," Phys. Rev. Lett. 127, 100401 (2021).